



Functional enzyme–polymer complexes

Curt Waltmann^a, Carolyn E. Mills^{b,1}, Jeremy Wang^{a,1}, Baofu Qiao^a, John M. Torkelson^{a,b}, Danielle Tullman-Ercek^b, and Monica Olvera de la Cruz^{a,b,c,d,2}

Contributed by Monica Olvera de la Cruz; received October 25, 2021; accepted February 21, 2022; reviewed by Andrew Spakowitz and Sarah Perry

Engineered and native enzymes are poised to solve challenges in medicine, bioremediation, and biotechnology. One important goal is the possibility of upcycling polymers using enzymes. However, enzymes are often inactive in industrial, nonbiological conditions. It is particularly difficult to protect water-soluble enzymes at elevated temperatures by methods that preserve their functionality. Through atomistic and coarse-grained molecular dynamics simulations that capture protein conformational change, we show that an enzyme, PETase (polyethylene terephthalate [PET]), can be stabilized at elevated temperatures by complexation with random copolymers into nanoscale aggregates that do not precipitate into macroscopic phases. We demonstrated the efficiency of the method by simulating complexes of random copolymers and the enzyme PETase, which depolymerizes PET, a highly used polymer. These polymers are more industrially viable than peptides and can target specific domains on an enzyme. We design the mean composition of the random copolymers to control the polymer–enzyme surface contacts and the polymer conformation. When positioned on or near the active site, these polymer contacts can further stabilize the conformation of the active site at elevated temperatures. We explore the experimental implications of this active site stabilization method and show that PETase-random copolymer complexes have enhanced activity on both small molecule substrates and solid PET films. These results provide guidelines for engineering enzyme–polymer complexes with enhanced enzyme functionality in nonbiological environments.

enzymes | complex coacervation | random copolymers | coarse-grained molecular simulations | GoMartini

Enzymes have the potential to tremendously impact the fields of pharmacology (1, 2), biotechnology (3), and bioremediation (4). They are especially useful for upcycling plastics (5), which are currently polluting oceans (6–8) and freshwater supplies harming both humans (9) and animals (10, 11). Enzymes such as lipases (12), cutinases (13, 14), hydrolases (15), and cytochrome P450 (16, 17) can catalyze a growing number of reactions due to advances in enzyme engineering (17, 18). In addition to engineering new catalytic functions, attempts have been made to increase enzyme efficiency by creating multienzyme complexes (19, 20), immobilizing them on two-dimensional surfaces (3, 16, 21–23), embedding them in plastics (4), and modifying the amino acid composition of enzymes to increase their thermal stability (24, 25). Stabilizing these enzymes is crucial for applications in nonbiological conditions such as elevated temperatures and pressures. Here, we investigate how complexation with random copolymers can enhance the high-temperature stability of the enzyme PETase (polyethylene terephthalate [PET]) (26), which degrades PET. PET is a glassy polymer at room temperature. Therefore, for PETase to function effectively, the temperature should be raised above T_g (70 °C) (27), which would normally denature the enzyme. Our simulations demonstrate the relationship between polymer composition and protein–polymer structure as well as the spatial correlations between chemically different monomers and the heterogeneous protein surface. We then show how the structure of the protein–polymer complex can impact the catalytic function of the enzyme, especially at elevated temperatures. Finally, we provide experimental verification of this enhanced catalytic activity of PETase in the presence of random copolymers.

Charged polymers have been used to encapsulate and stabilize proteins through either macroscopic segregation (28, 29) or microphase separation into nanoscale aggregates that do not precipitate into macroscopic phases (15, 30, 31). This approach works on a wide variety of proteins including engineered proteins with nonbiological functions (17, 32), because protein–polymer interactions can be altered in many ways to enhance complexation (33, 34) including by modifying the charge of the proteins themselves (35, 36). Phase separation through engineering protein charge distribution has also been demonstrated *in vivo* (37) in cellular bodies known as membraneless organelles (38) (MLOs). MLOs are composed of proteins, nucleic acids, and small molecule metabolites (39) and are often formed from intrinsically disordered proteins (IDPs) or proteins with intrinsically disordered regions (IDRs). IDPs control the MLO composition based

Significance

The use of biological enzyme catalysts could have huge ramifications for chemical industries. However, these enzymes are often inactive in nonbiological conditions, such as high temperatures, present in industrial settings. Here, we show that the enzyme PETase (polyethylene terephthalate [PET]), with potential application in plastic recycling, is stabilized at elevated temperature through complexation with random copolymers. We demonstrate this through simulations and experiments on different types of substrates. Our simulations also provide strategies for designing more enzymatically active complexes by altering polymer composition and enzyme charge distribution.

Author affiliations: ^aDepartment of Materials Science and Engineering, Northwestern University, Evanston, IL 60208; ^bDepartment of Chemical and Biological Engineering, Northwestern University, Evanston, IL 60208; ^cDepartment of Chemistry, Northwestern University, Evanston, IL 60208; and ^dDepartment of Physics and Astronomy, Northwestern University, Evanston, IL 60208

Author contributions: C.W., C.E.M., J.W., B.Q., J.M.T., D.T.-E., and M.O.d.I.C. designed research; C.W., C.E.M., and J.W. performed research; C.W., C.E.M., J.W., B.Q., and M.O.d.I.C. analyzed data; and C.W., C.E.M., J.W., B.Q., J.M.T., D.T.-E., and M.O.d.I.C. wrote the paper.

Reviewers: A.J.S., Stanford University; and S.P., University of Massachusetts Amherst.

The authors declare no competing interest.

Copyright © 2022 the Author(s). Published by PNAS. This article is distributed under [Creative Commons Attribution-NonCommercial-NoDerivatives License 4.0 \(CC BY-NC-ND\)](https://creativecommons.org/licenses/by-nc-nd/4.0/).

¹C.E.M. and J.W. contributed equally to this work.

²To whom correspondence may be addressed. Email: m-olvera@northwestern.edu.

This article contains supporting information online at <https://www.pnas.org/lookup/suppl/doi:10.1073/pnas.2119509119/-DCSupplemental>.

Published March 21, 2022.

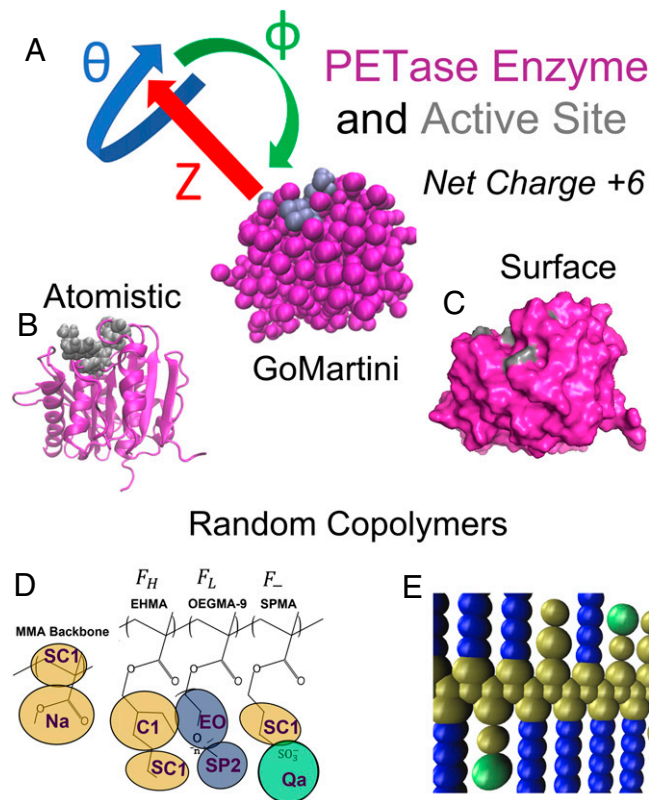


Fig. 1. Description and models of PETase and the random copolymers. (A) GoMartini model of PETase in magenta with the active site in gray. (B) The secondary structure of PETase is shown with the same color scheme as in A. The active site is shown using the van der Waals representation to highlight the left-like binding pocket for PET. (C) Surface representation of PETase. (D) Chemical and Martini description of the methacrylate-based random copolymers. Hydrophobic beads are tan, while hydrophilic beads are blue, and negatively charged beads are cyan. F_H , F_L , and F_- refer to the percentage of the respective monomer in the random copolymers. (E) Snapshot of the Martini random copolymer model with the colors corresponding to D.

on specific interactions that originate from the IDP sequence (40) and this spatial organization helps to regulate the internal biochemistry of cells. Inspired by IDPs, we design a microphase separated protein–polymer complex using random copolymers. These random copolymers contain monomers with a common backbone but different side chains that can be polar, nonpolar, or charged. The monomers, shown in Fig. 1 D and E, are oligo-ethyl glycol methacrylate with a length of nine ethyl glycol units (OEGMA-9), ethyl hexyl methacrylate (EHMA), and sulfo-propyl methacrylate (SPMA). Due to their methyl methacrylate backbone, they are inexpensive to randomly polymerize in large-scale, industrial processes. They have also been used in previous computational and experimental studies of polymer complexes with proteins including horseradish peroxidase, glucose oxidase, and organophosphorus hydrolase as well as small organic molecules (32, 41). Further, amphiphilic random copolymers are well suited to complex with the heterogeneous polar and nonpolar surfaces of proteins (42) including PETase. Thus, in addition to the electrostatic attraction between the polymer and protein, the polar and nonpolar groups of the random copolymers can self-optimize (43), maximizing their interactions with protein surface domains, making this complexation quite general (32, 42, 44).

In the present study, we explore how complexation with random copolymers can affect the conformation, and thus the function, of PETase especially at temperatures the enzyme does not experience in vivo. We achieve this by varying the mean polymer

composition, which controls the polymer–protein surface interactions. This, in turn, affects complex formation and the spatial distribution of contacts on the surface of the enzyme. While there have been previous studies of protein–polymer complexation (33, 45), experimental studies are inherently limited in the direct observation of surface correlations (46) and previous computational studies have used coarse models that did not include charges (42) or vary the mean composition (32). Other models (47) were used to study PETase and cytochrome P450 in the context of macroscopic complexes instead of nanoscale complexes and they were also unable to study the effect of the polymers on the conformation of the enzyme active site, which we show is affected by the spatial distribution of protein–polymer contacts at both room and elevated temperatures. Specifically, we demonstrate that when these PETase–random copolymer complexes have an abundance of polymer–active site contacts, they can have less perturbed active sites than the protein by itself and remain stable as the temperature is increased.

1. Results and Discussion

A. PETase Structure at Elevated Temperature. PETase denatures as temperature is increased, leading to detectable decreases in activity above room temperature (24, 25). In Fig. 2A, all-atom molecular dynamics simulations demonstrate the deformation of the active site at elevated temperatures. We use protein rmsd (48) to measure the conformation of the protein relative to the energy-minimized crystal structure, not including rotational or translational diffusion. We measure the conformation of the whole protein as well as the active site using a previously published definition of the seven active site residues (26). This provides metrics for the behavior of the whole protein and the active site, whose conformation relative to the crystal structure correlates with enzymatic activity (49).

As shown in Fig. 2A, there is an upward trend for both the whole protein and active site rmsd values as the temperature increases and PETase activity decreases. The active site rmsd at 330 K is an outlier—despite decreasing from 320 K, it is still higher than 298 or 310 K. In agreement with studies highlighting the flexibility of the active site (49), we see that the active site is more perturbed by increases in temperature (especially at the

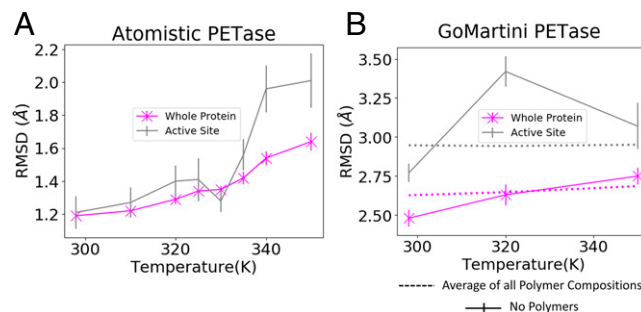


Fig. 2. (A and B) Comparison of the GoMartini PETase (B) alone to atomistic simulations (A) and to the GoMartini PETase complexed with random copolymers as the temperature is increased (B). rmsd is used to measure the conformation relative to the crystal structure with higher values signifying more deformation. (A) Results for the atomistic model show a general increase in the rmsd of the protein as well as the active site as is expected based on known decreases in activity with increasing temperature. (B) The GoMartini model shows an increase in rmsd for the whole protein and the active site at 320 K, but at 350 K the active site rmsd decreases, unlike the entire protein backbone. The active site rmsd may be inaccurate at high temperatures, but can still be used as a baseline to measure the thermal stability of the PETase–polymer complexes. In these complexes, temperature dependence of the whole protein and active site conformation is nearly eliminated.

highest temperatures) when compared to the whole protein. In the following sections where random copolymers complex with PETase, we use the GoMartini (50) model of PETase, which agrees reasonably well with the temperature-dependent conformation of atomistic PETase (Fig. 2A). As shown in Fig. 2B, the GoMartini PETase also shows an upward trend for both rmsd values with temperature as well as larger increases for the active site than for the whole protein. Although the rmsd values are different between the atomistic and GoMartini models, they are also measured on different time scales, 10 ns for the atomistic results and 300 ns for the GoMartini results (see *SI Appendix, Materials and Methods* for more details), with longer times potentially leading to further perturbation of the protein structure. The ability to access these longer time scales is a great advantage of the GoMartini model. In agreement with atomistic simulations, the GoMartini model does have a noticeable increase at 320 K. However, at 350 K, the active site rmsd decreases instead of increasing. Here, the model is failing to accurately predict the active site behavior of PETase, although the whole protein rmsd displays the correct trend. Despite this issue, the GoMartini model still provides a baseline that can be compared to the case of polymer complexation to evaluate the ability of the polymers to stabilize the active site. This issue is also mitigated by restricting our analysis of the active site to 320 K in some cases (see Fig. 6C).

B. Enzyme-Polymer Complexation. Since the stabilization of enzymes through microphase complexation depends on the structure of the adsorbed random copolymers, we seek to understand how to control the adsorption through mean composition of the polymer. We measure the adsorption via the number of contacts between the polymer and the enzyme at three temperatures. The results at 298 K are shown in Fig. 3. The trends observed at this temperature continue at higher temperatures (*SI Appendix, Fig. S1*).

A Total Normalized Polymer-PETase Contacts

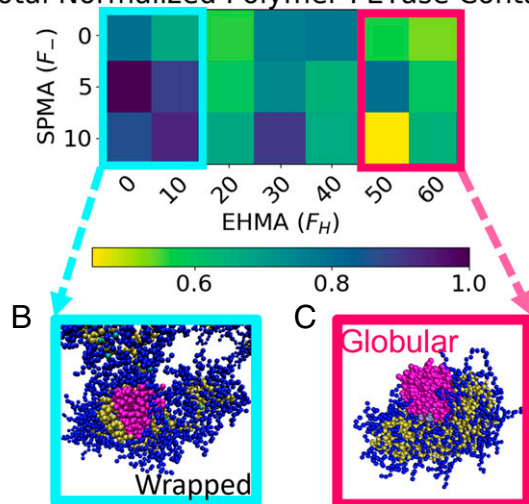


Fig. 3. Random copolymer complexation with the PETase protein for different mean polymer compositions. F_H is the percentage of hydrophobic EHMA, F_- is the percentage of negatively charged SPMA, and F_L is the percentage of hydrophilic OEGMA-9. These percentages sum to 100 and thus F_L , which is not displayed, is $100 - F_H - F_-$. (A) The number of contacts is shown as a function of composition at 298 K. A maximum is observed at very low percentages of EHMA and higher percentages of SPMA, while a local minimum is observed at $F_H = 20\%$. (B) Simulation snapshot of a wrapped polymer conformation, which occurs at low values of F_H and is characterized by a high percentage of contacts between the enzyme and polymer backbone. (C) Simulation snapshot of a globular polymer conformation, which occurs at high values of F_H and is characterized by micelle-like behavior of the amphiphilic polymers.

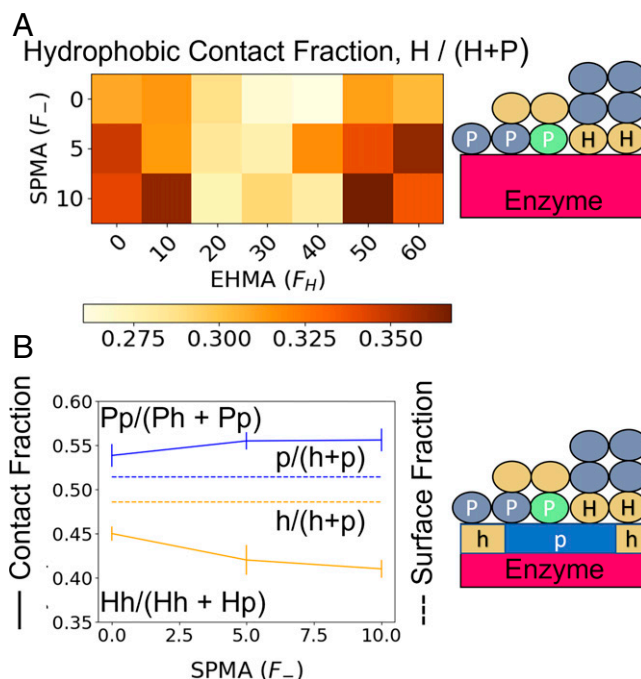


Fig. 4. Hydrophobic interactions affect PETase-random copolymer complexation. (A) The fraction of contacts that involve hydrophobic polymer beads. There are two local maxima, one at very low F_H where the polymer backbone wraps around the protein surface and one at high F_H where the EHMA increases the baseline hydrophobic fraction of the polymer. (B) The fraction of these hydrophobic contacts that occur on the hydrophobic surface of PETase is lower than the hydrophobic surface fraction of PETase. This struggle to optimize the interaction could be related to ill-defined hydrophobic domains due to partially hydrophobic amino acids in the Martini model. However, polar-polar interactions seem to be optimized and this increases as charge is added, while the opposite occurs for hydrophobic-hydrophobic interactions.

As shown in Fig. 3A, the mean compositions with the most contacts between polymers and protein tend to be those with a relatively high percentage of negatively charged SPMA, F_- , and a lower percentage of hydrophobic EHMA, F_H . Thus, additional hydrophobic EHMA monomers are unnecessary for the polymer to complex with the hydrophobic domains of the protein surface since the polymer backbone is already hydrophobic.

This is further illustrated in Fig. 4A by the fraction of protein-polymer contacts that involve a hydrophobic polymer bead either from the backbone of the polymer or from the side chains. Local maxima of the fraction of hydrophobic contacts occur at both the highest and the lowest values of F_H . These low F_H conformations wrap around the PETase surface (Fig. 3B), as opposed to higher F_H compositions that lead to globular polymer conformations (Fig. 3C). Thus, the wrapped conformation of the low F_H random copolymers allows the hydrophobic backbone to more easily access the protein surface, leading to more hydrophobic and total protein-polymer contacts. The connectivity of the hydrophobic backbone and hydrophobic globular conformations seems to lead to the creation of contacts with both the polar and hydrophobic parts of the protein as shown by the weaker hydrophobic correlations between polymer and protein (Fig. 4B). The polar correlations are stronger, possibly due to reduced connectivity of the polar side chains and the ability to interact with the aqueous solvent instead of the protein surface. We note this analysis is highly sensitive to how the hydrophobicity of different beads is defined (*SI Appendix, sections B.3 and C.3*).

The number of polymer-enzyme contacts grew as F_- increased, especially for wrapped conformations. This increased attraction between the enzyme and the random copolymers is

Additional Contacts (ACs) of Negatively Charged Polymers Are Located on Positive Protein Domains

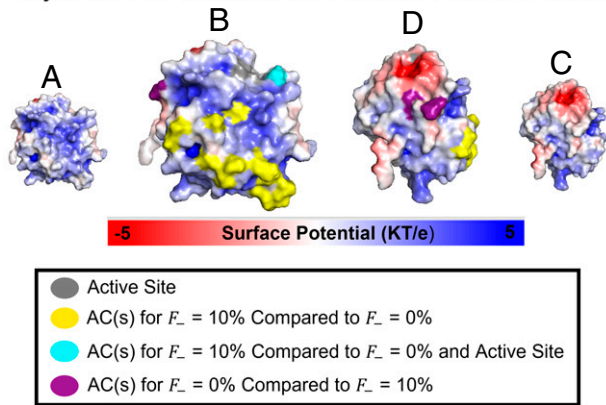


Fig. 5. Including negatively charged monomers increases contact with positive surface domains. (A and B) PETase with only the surface potential and with additional contacts (ACs) overlaid, respectively. One can see that the yellow and cyan sites, which are preferred when $F_- = 10\%$, are overwhelmingly on the positive part of the protein due to the addition of negative charge to the polymer. (C and D) A rotated orientation of the protein. The full dataset for this, more method description, and higher-temperature results can be found in *SI Appendix, Fig. S2*.

intuitive since PETase has a +6 net charge. The increase in contacts occurs on the positively charged part of the surface as shown in Fig. 5. Thus, the charge of the polymer influences the spatial distribution of the polymer on the dipolar PETase surface (26) and the overall number of contacts. There is also some competition between optimizing charged and hydrophobic interactions as the addition of charge slightly weakens the hydrophobic correlations (Fig. 4B). These contacts were biased to a specific protein domain despite the randomness of the polymer sequence, suggesting that using more controlled polymerization or peptide engineering is not necessary to intentionally contact these charged domains. It also suggests that the inverse can be achieved; i.e., a certain protein domain could be targeted by engineering the surface potential. Experiments have also demonstrated that protein charge domains are crucial in macrophase behavior of protein–polyelectrolyte complexes (29, 45). This is also true of polymer blockiness (51–53), or the tendency of like monomers to be grouped together in the polymer sequence, in phase separation of polyelectrolyte complexes especially as ionic conditions are varied (54–56).

C. Stability of the Complexed Enzyme. In Fig. 2B, we measure how complexation affects the conformation of the protein at room and elevated temperatures, using the rmsd values for the protein and the active site. These rmsd values are a measure of the protein conformation relative to the PETase crystal structure with lower values representing less perturbed active sites and thus a more active enzyme.

We find that the random copolymers are very effective at preventing PETase from deforming as the temperature is increased. This is shown by the rmsd values for the active site and the whole protein averaged over all polymer compositions and compared with the results for PETase without polymers (Fig. 2B). The rmsd values as a function of temperature with polymers bound are almost flat for the whole protein and the active site; the actual values for the active site and the whole protein are only slightly greater than those for the protein alone at 298 K. The perturbations caused by polymer binding are less than the perturbations seen at elevated temperatures as at 320 K. Thus, the stability of the active site is much improved with the addition of polymers. The distribution of active site rmsd values at 320 K shows that for nearly

every polymer composition the active site rmsd is lower than that without polymers (*SI Appendix, Fig. S3A*). The rmsd values for the active site also have a much broader range when compared to the values of the whole protein (*SI Appendix, Fig. S3B*). Further, this range includes some active site rmsd values that are lower at room temperature with polymers than without. This wide range of rmsd values for the active site is not well explained by trends in mean polymer composition (*SI Appendix, Fig. S4*). To explain the wide range of active site behavior we look at the location of the contacts for those compositions where active sites are less perturbed than the PETase alone at room temperature and compare to compositions where active sites are more perturbed than the PETase alone at room temperature (Fig. 6). We find that less perturbed compositions have significantly more contacts near or on the active site of the enzyme at both 298 K (Fig. 6C) and 320 K (Fig. 6D). This suggests that contacts on the active site stabilize instead of perturb the active site. Thus, although we found a correlation between polymer contacts on the positive section of the enzyme and mean polymer composition in Fig. 5, these contacts were not concentrated on the active site, which explains the absence of correlation between mean polymer composition and active site conformation (*SI Appendix, Fig. S4*). In other words, the composition of the polymers (especially charge) biases the spatial distribution of contacts, but it does not bias these contacts to the active site, where they provide stability. This does not necessarily have to be the case for PETase or any given enzyme, since previous work has shown that complexation can be influenced by engineering the net charge on various proteins (35, 36). A similar strategy could be used to change the charge distribution near the active site. Thus, we suggest that engineering the spatial distribution of charges near the active site could increase the activity of an enzyme–polymer complex by biasing the charged polymers near the active site and stabilizing the active site. While

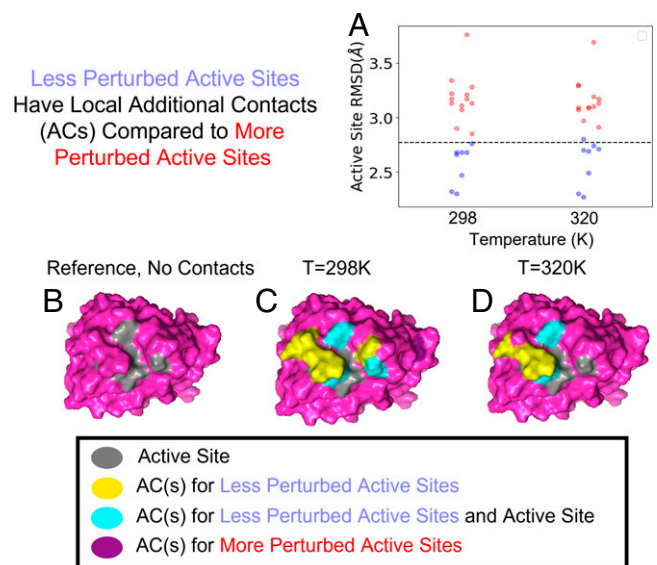


Fig. 6. Less perturbed active sites are stabilized by additional contacts near the active site. (A) The distribution of active site rmsds at 298 and 320 K. The less perturbed active sites are colored in blue while the more perturbed active sites are colored in red. Each point refers to a different polymer composition and the line refers to PETase alone at 298 K. These are the groups being compared in C and D. (B) Surface representation of PETase with no excess contacts shown for comparison. (C) Comparison at 298 K shows many ACs around the active sites for less perturbed compositions. These contacts stabilize the active site instead of further perturbing it at 320 K (D) as well. The full dataset for this and more method description can be found in *SI Appendix, Fig. S6*.

active site stabilization due to local contacts may not be completely general, previous studies have illustrated that the addition of polymers to enzymes can enhance the activity at elevated temperatures in water (15, 57), suggesting the phenomenon extends beyond PETase. Moreover, most active sites are partially hydrophobic (58–61), suggesting that polymers with hydrophobic groups can stabilize the active site with local contacts as shown here.

D. Activity of Enzyme–Polymer Complexes on Small Molecule and Solid Substrates. We performed experiments to assess the impact of active site stabilization on enzyme activity. We first examined the temperatures at which our PETase/copolymer complexes are stable. We incubated PETase or PETase/copolymer mixtures at a range of temperatures (4 to 50 °C) for 1 h and assayed esterase activity at room temperature against the small molecule substrate, p-nitrophenyl acetate (Fig. 7A). Here, we used a small molecule substrate to avoid confounding effects of temperature on PETase’s PET degrading activity (an established phenomenon) (24, 25). The copolymer used in these studies has a mean composition with $F_H = 43\%$ and $F_- = 12\%$, within the normal range of F_H in the simulations and a reasonably similar value of F_- (see *Materials and Methods* for further detail). Interestingly, we found that for all incubation temperatures, the specific esterase activity of PETase was enhanced in the presence of copolymer and that this activity enhancement increased at higher copolymer concentrations (Fig. 7A). Our data also indicate that PETase activity in PETase/copolymer complexes is stable at temperatures up to 40 °C. Notably, this is less than the glass transition temperature of PET (70 °C). While the activity enhancement with the addition of copolymer could improve the utility of the enzyme, further thermal stabilization of the PETase enzyme is likely needed to realize the full potential of this system. For example, polymers with side groups that penetrate PET could be used to decrease its T_g .

Next, we examined the activity of PETase/copolymer complexes on solid PET as a substrate over 5 h at 35 °C (Fig. 7B). The presence of copolymer enhances the activity of PETase toward PET, similar to the results obtained with our small molecule activity assay. We confirmed that none of the formulations tested exhibited any decrease in esterase activity after incubation at 35 °C for 5 h (*SI Appendix*, Fig. S8), suggesting that the enhanced enzyme activity with copolymer is not due to changes in the temporal stability of the enzyme. Thus, our experimental data suggest that PETase activity is improved upon addition of copolymer regardless of the substrate. These results, in conjunction with our simulation studies, suggest that copolymer binding impacts

active site conformation, thus altering PETase activity. We observe a wide distribution of active site conformations in simulations in the presence of copolymer compared to the naked enzyme (Fig. 2C). While some of these active site conformations may be less active than the native enzyme, we hypothesize that there may be a few active conformations present at any given time that confer substantially higher enzyme activity. An alternative hypothesis is that the random copolymers interact favorably with the substrate, leading to an increase in local substrate concentration. Indeed, it has been shown that these random copolymers can bind hydrophobic small molecules (41) and that IDRs in proteins, similar to the random copolymers in Fig. 4B, promote higher-order assembly (62). However, because the increase in PETase activity appears to be independent of substrate (solid PET or aqueous p-nitrophenyl acetate), it is more likely that the interactions responsible for this activity enhancement are between the PETase and the random copolymer rather than the random copolymer and the substrate.

2. Conclusions and Outlook

The ability to use various types of enzymes in industrial conditions could dramatically impact biotechnology, pharmacology, and bioremediation. Here, we show the following: 1) PETase is functionally stabilized by complexation with industrially scalable random copolymers. We demonstrate this through simulations of whole protein and active site conformations and using experiments measuring enzyme activity in response to thermal challenge. 2) This effect is further enhanced when random copolymers form more contacts with the enzyme active site. 3) Polymer composition biases the conformation and location of the random copolymers on a protein despite the randomness of the polymer sequences. Thus, engineering the surface potential of the protein, using standard protein mutation or modification techniques, could bias polymers to bind near the active site, further increasing enzyme activity. This approach may be compatible with a variety of enzymes as long as their surfaces can be engineered without misfolding. However, the use of copolymer complexation to modify active site conformation does not necessitate further protein mutation or modification as the diverse functional groups on the copolymer should permit binding to a variety of protein surfaces. Further, this approach can also be used in the absence of information on the sequence and structure of an enzyme. Thus, this strategy has the potential to be a widely accessible route to increasing enzyme functionality, especially given that it requires only a random polymerization. Future experiments using substrates with various physical properties could elucidate the role of interactions between substrates and random copolymers, opening another avenue for engineering enzyme activity via complexation with copolymers. These interactions could be controlled by using monomers with specific affinities and promote assembly on solid substrates like PET films.

Complexation with random copolymers is a welcome addition to the enzyme engineering toolbox, offering an orthogonal, versatile strategy for increasing functionality either in conjunction with or independent of other protein engineering techniques.

Materials and Methods

Copolymer Production and Purification. The random copolymer used in this study was synthesized and purified as described in *SI Appendix*. Based on previous work with the same monomer set showing that reactivity ratios of these monomers are close to 1, we assume ideal random incorporation (32).

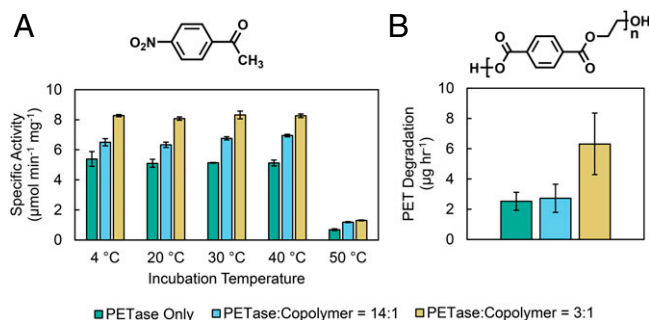


Fig. 7. Activity of PETase and PETase/copolymer complexes at two different PETase:copolymer molar ratios. (A) Specific activity against small molecule substrate p-nitrophenyl acetate after 1 h incubation at various temperatures. Error bars represent SD over three replicate experiments. (B) PET degradation activity over 5 h at 35 °C. Error bars represent the 95% confidence interval on activity values.

The polymer was characterized by gel permeation chromatography (GPC) and hydrogen NMR (HNMR) and found to be 170 kDa ($D=1.3$), with 45% OEGMA-9, 43% EHMA, and 12% SPMA, mol/mol. Details of these characterizations can be found in [SI Appendix](#).

Protein Production. PETase was expressed and purified as described in [SI Appendix](#).

PETase Activity after Thermal Challenge. PETase and PETase/random copolymer samples were prepared as described in [SI Appendix](#). These samples were either refrigerated at 4 °C or incubated in a Bio-Rad C1000 thermal cycler set to the specified temperature (20, 30, 40, or 50 °C) for 1 h. Samples were then brought to room temperature and assayed for esterase activity using small molecule substrate p-nitrophenyl acetate as described in [SI Appendix](#).

PETase Activity on PET Films. PETase and PETase/random copolymer solutions were prepared in 20-mL glass scintillation vials as described in [SI Appendix](#). To measure PET degradation, PET discs 0.2 mm thick and 1.27 cm in diameter were submerged in the PETase-containing solutions and incubated at 35 °C for

1 to 5 h. MHET production in each vial was determined by measuring solution absorbance at 242 nm. Further details can be found in [SI Appendix](#).

Data Availability. All study data are included in this article and/or [SI Appendix](#).

ACKNOWLEDGMENTS. We thank the the Department of Energy, Office of Basic Energy Sciences for financial support under Contract DE-FG02-08ER46539. M.O.d.I.C. thanks the Sherman Fairchild Foundation for computational support. C.W., B.O., J.W., and M.O.d.I.C. thank the Center for Computation and Theory of Soft Materials for support. B.O. was funded by the Center for Hierarchical Materials Design. J.M.T., M.O.d.I.C., C.E.M. and D.T.-E. were funded by a Cornew Innovation Award through the Chemistry of Life Processes Institute at Northwestern University. This work made use of the Integrated Molecular Structure Education and Research Center NMR facility at Northwestern University, which has received support from the Soft and Hybrid Nanotechnology Experimental Resource (NSF ECCS-2025633) and Northwestern University. This work also made use of the Keck Biophysics Facility (aqueous GPC) at Northwestern University, which is supported by the Robert H. Lurie Comprehensive Cancer Center (National Cancer Institute P30 Cancer Center Support Grant CA060553).

1. M. J. Coon, Cytochrome P450: Nature's most versatile biological catalyst. *Annu. Rev. Pharmacol. Toxicol.* **45**, 1–25 (2005).
2. C. A. Martínez, S. G. Rupasinghe, Cytochrome P450 bioreactors in the pharmaceutical industry: Challenges and opportunities. *Curr. Top. Med. Chem.* **13**, 1470–1490 (2013).
3. H. V. Sureka, A. C. Obermeyer, R. J. Flores, B. D. Olsen, Catalytic biosensors from complex coacervate core micelle (c3m) thin films. *ACS Appl. Mater. Interfaces* **11**, 32354–32365 (2019).
4. C. DelRe *et al.*, Near-complete depolymerization of polyesters with nano-dispersed enzymes. *Nature* **592**, 558–563 (2021).
5. L. M. Blank, T. Narancic, J. Mampel, T. Tiso, K. O'Connor, Biotechnological upcycling of plastic waste and other non-conventional feedstocks in a circular economy. *Curr. Opin. Biotechnol.* **62**, 212–219 (2020).
6. A. Cózar *et al.*, Plastic debris in the open ocean. *Proc. Natl. Acad. Sci. U.S.A.* **111**, 10239–10244 (2014).
7. K. L. Law *et al.*, Plastic accumulation in the North Atlantic subtropical gyre. *Science* **329**, 1185–1188 (2010).
8. J. R. Jambeck *et al.*, Marine pollution. Plastic waste inputs from land into the ocean. *Science* **347**, 768–771 (2015).
9. K. D. Cox *et al.*, Human consumption of microplastics. *Environ. Sci. Technol.* **53**, 7068–7074 (2019).
10. J. B. Lamb *et al.*, Plastic waste associated with disease on coral reefs. *Science* **359**, 460–462 (2018).
11. I. A. Kane *et al.*, Seafloor microplastic hotspots controlled by deep-sea circulation. *Science* **368**, 1140–1145 (2020).
12. A. Su *et al.*, Cutinases as stereoselective catalysts: Specific activity and enantioselectivity of cutinases and lipases for menthol and its analogs. *Enzyme Microb. Technol.* **133**, 109467 (2020).
13. A. N. Shirke *et al.*, Stabilizing leaf and branch compost cutinase (lcc) with glycosylation: Mechanism and effect on pet hydrolysis. *Biochemistry* **57**, 1190–1200 (2018).
14. A. M. Ronkvist, W. Xie, W. Lu, R. A. Gross, Cutinase-catalyzed hydrolysis of poly(ethylene terephthalate). *Macromolecules* **42**, 5128–5138 (2009).
15. C. E. Mills, A. Obermeyer, X. Dong, J. Walker, B. D. Olsen, Complex coacervate core micelles for the dispersion and stabilization of organophosphate hydrolase in organic solvents. *Langmuir* **32**, 13367–13376 (2016).
16. S. B. Lamb, D. C. Lamb, S. L. Kelly, D. C. Stuckey, Cytochrome P450 immobilisation as a route to bioremediation/biocatalysis. *FEBS Lett.* **431**, 343–346 (1998).
17. K. Chen, F. H. Arnold, Engineering cytochrome p450s for enantioselective cyclopropanation of internal alkenes. *J. Am. Chem. Soc.* **142**, 6891–6895 (2020).
18. F. H. Arnold, Directed evolution: Bringing new chemistry to life. *Angew. Chem. Int. Ed. Engl.* **57**, 4143–4148 (2018).
19. N. C. Dubej, B. P. Tripathi, Nature inspired multienzyme immobilization: Strategies and concepts. *ACS Appl. Bio Mater.* **4**, 1077–1114 (2021).
20. B. C. Knott *et al.*, Characterization and engineering of a two-enzyme system for plastics depolymerization. *Proc. Natl. Acad. Sci. U.S.A.* **117**, 25476–25485 (2020).
21. L. A. Wollenberg *et al.*, The use of immobilized cytochrome P450C9 in PMMA-based plug flow bioreactors for the production of drug metabolites. *Appl. Biochem. Biotechnol.* **172**, 1293–1306 (2014).
22. J. Ducharme, K. Auclair, Use of bioconjugation with cytochrome P450 enzymes. *Biochim. Biophys. Acta. Proteins Proteomics* **1866**, 32–51 (2018).
23. A. Su, A. Shirke, J. Baik, Y. Zou, R. Gross, Immobilized cutinases: Preparation, solvent tolerance and thermal stability. *Enzyme Microb. Technol.* **116**, 33–40 (2018).
24. H. F. Son *et al.*, Rational protein engineering of thermo-stable PETase from *Ideonella sakaiensis* for highly efficient PET degradation. *ACS Catal.* **9**, 3519–3526 (2019).
25. Y. Cui *et al.*, Computational redesign of a PETase for plastic biodegradation under ambient condition by the GRAPE strategy. *ACS Catal.* **11**, 1340–1350 (2021).
26. H. P. Austin *et al.*, Characterization and engineering of a plastic-degrading aromatic polyesterase. *Proc. Natl. Acad. Sci. U.S.A.* **115**, E4350–E4357 (2018).
27. J. P. Jog, Crystallization of polyethyleneterephthalate. *J. Macromol. Sci. Part C* **35**, 531–553 (1995).
28. X. Mi *et al.*, Thermostabilization of viruses via complex coacervation. *Biomater. Sci.* **8**, 7082–7092 (2020).
29. W. C. Blocher McGigue, S. L. Perry, Design rules for encapsulating proteins into complex coacervates. *Soft Matter* **15**, 3089–3103 (2019).
30. A. C. Obermeyer, C. E. Mills, X. H. Dong, R. J. Flores, B. D. Olsen, Complex coacervation of supercharged proteins with polyelectrolytes. *Soft Matter* **12**, 3570–3581 (2016).
31. J. M. Horn, R. A. Kapelner, A. C. Obermeyer, Macro- and microphase separated protein-polyelectrolyte complexes: Design parameters and current progress. *Polymers (Basel)* **11**, 578 (2019).
32. B. Panganiban *et al.*, Random heteropolymers preserve protein function in foreign environments. *Science* **359**, 1239–1243 (2018).
33. R. A. Kapelner, V. Yeong, A. C. Obermeyer, Molecular determinants of protein-based coacervates. *Curr. Opin. Colloid Interface Sci.* **52**, 101407 (2021).
34. A. Huang *et al.*, Predicting protein-polymer block copolymer self-assembly from protein properties. *Biomacromolecules* **20**, 3713–3723 (2019).
35. R. A. Kapelner, A. C. Obermeyer, Ionic polypeptide tags for protein phase separation. *Chem. Sci. (Camb.)* **10**, 2700–2707 (2019).
36. C. E. Cummings, A. C. Obermeyer, Phase separation behavior of supercharged proteins and polyelectrolytes. *Biochemistry* **57**, 314–323 (2018).
37. V. Yeong, E. G. Werth, L. M. Brown, A. C. Obermeyer, Formation of biomolecular condensates in bacteria by tuning protein electrostatics. *ACS Cent. Sci.* **6**, 2301–2310 (2020).
38. S. F. Banani, H. O. Lee, A. A. Hyman, M. K. Rosen, Biomolecular condensates: Organizers of cellular biochemistry. *Nat. Rev. Mol. Cell Biol.* **18**, 285–298 (2017).
39. T. J. Nott *et al.*, Phase transition of a disordered nuage protein generates environmentally responsive membraneless organelles. *Mol. Cell* **57**, 936–947 (2015).
40. C. W. Pak *et al.*, Sequence determinants of intracellular phase separation by complex coacervation of a disordered protein. *Mol. Cell* **63**, 72–85 (2016).
41. J. Wang, C. Waltmann, H. Umana-Kossio, M. Olvera de la Cruz, J. M. Torkelson, Heterogeneous charged complexes of random copolymers for the segregation of organic molecules. *ACS Cent. Sci.* **7**, 882–891 (2021).
42. T. D. Nguyen, B. Qiao, M. Olvera de la Cruz, Efficient encapsulation of proteins with random copolymers. *Proc. Natl. Acad. Sci. U.S.A.* **115**, 6578–6583 (2018).
43. S. Mao, Q. J. MacPherson, S. S. He, E. Coletta, A. J. Spakowitz, Impact of conformational and chemical correlations on microphase segregation in random copolymers. *Macromolecules* **49**, 4358–4368 (2016).
44. B. Qiao, F. Jiménez-Ángeles, T. D. Nguyen, M. Olvera de la Cruz, Water follows polar and nonpolar protein surface domains. *Proc. Natl. Acad. Sci. U.S.A.* **116**, 19274–19281 (2019).
45. S. Kim *et al.*, Effect of protein surface charge distribution on protein-polyelectrolyte complexation. *Biomacromolecules* **21**, 3026–3037 (2020).
46. C. DelRe *et al.*, Rational design of a synthetic peg-like polymer for protein stabilization. *J. Phys. J.* **112**, 59a (2017).
47. A. Cardellini, F. Jiménez-Ángeles, P. Asinari, M. Olvera de la Cruz, A modeling-based design to engineering protein hydrogels with random copolymers. *ACS Nano* **15**, 16139–16148 (2021).
48. V. N. Maiorov, G. M. Crippen, Size-independent comparison of protein three-dimensional structures. *Proteins* **22**, 273–283 (1995).
49. T. Fecker *et al.*, Active site flexibility as a hallmark for efficient pet degradation by *I. sakaiensis* petase. *Biophys. J.* **114**, 1302–1312 (2018).
50. A. B. Poma, M. Cieplak, P. E. Theodorakis, Combining the MARTINI and structure-based coarse-grained approaches for the molecular dynamics studies of conformational transitions in proteins. *J. Chem. Theory Comput.* **13**, 1366–1374 (2017).
51. A. M. Romyantsev *et al.*, Controlling complex coacervation via random polyelectrolyte sequences. *ACS Macro Lett.* **8**, 1296–1302 (2019).
52. T. K. Lytle, L. W. Chang, N. Markiewicz, S. L. Perry, C. E. Sing, Designing electrostatic interactions via polyelectrolyte monomer sequence. *ACS Cent. Sci.* **5**, 709–718 (2019).
53. C. E. Sing, S. L. Perry, Recent progress in the science of complex coacervation. *Soft Matter* **16**, 2885–2914 (2020).
54. M. Ghasemi, S. Friedowitz, R. G. Larson, Analysis of partitioning of salt through doping of polyelectrolyte complex coacervates. *Macromolecules* **53**, 6928–6945 (2020).
55. M. Ghasemi, R. G. Larson, Role of electrostatic interactions in charge regulation of weakly dissociating polyacids. *Prog. Polym. Sci.* **112**, 101322 (2021).
56. S. Friedowitz, A. Salehi, R. G. Larson, J. Qin, Role of electrostatic correlations in polyelectrolyte charge association. *J. Chem. Phys.* **149**, 163335 (2018).
57. M. Kim *et al.*, Enhanced activity and stability of organophosphorus hydrolase via interaction with an amphiphilic polymer. *Chem. Commun. (Camb.)* **50**, 5345–5348 (2014).
58. D. Blaha-Nelson, D. M. Krüger, K. Szeler, M. Ben-David, S. C. L. Kamerlin, Active site hydrophobicity and the convergent evolution of paraoxonase activity in structurally divergent enzymes: The case of serum paraoxonase 1. *J. Am. Chem. Soc.* **139**, 1155–1167 (2017).
59. W. B. L. Alkema, A. J. Dijkhuis, E. De Vries, D. B. Janssen, The role of hydrophobic active-site residues in substrate specificity and acyl transfer activity of penicillin acylase. *Eur. J. Biochem.* **269**, 2093–2100 (2002).
60. P. W. Snyder *et al.*, Mechanism of the hydrophobic effect in the biomolecular recognition of arylsulfonamides by carbonic anhydrase. *Proc. Natl. Acad. Sci. U.S.A.* **108**, 17889–17894 (2011).
61. S. Goswami, S. Das, S. Datta, Understanding the role of residues around the active site tunnel towards generating a glucose-tolerant β -glucosidase from *Agrobacterium tumefaciens* SA. *Protein Eng. Des. Sel.* **30**, 523–530 (2017).
62. C. Waltmann, R. Asor, U. Raviv, M. Olvera de la Cruz, Assembly and stability of simian virus 40 polymorphs. *ACS Nano* **14**, 4430–4443 (2020).